JOURNAL OF GEOPHYSICAL RESEARCH, VOL. 92, NO. B9, PAGES 9215-9223, AUGUST 10, 1987

SLOW WAVES TRAPPED IN A FLUID-FILLED INFINITE CRACK: IMPLICATION FOR VOLCANIC TREMOR

Valerie Ferrazzini and Keiiti Aki

Department of Geological Sciences, University of Southern California, Los Angeles

Abstract. The dynamics and seismic radiation of fluid-filled cracks have been studied by numerous authors, as models for tremor and for long-period events observed at volcanoes. One of the most intriguing results of the recent models is the existence of a very slow wave propagating along the crack boundary. In order to better understand this slow wave, which has so far only been studied numerically, we studied analytically normal modes trapped in a liquid layer sandwiched between two solid half-spaces. A slow wave, similar to the tube wave found by Biot, exists for all wavelengths. In the short wavelength limit, this wave approaches the Stoneley wave for the liquid-solid interface. Unlike the tube wave, however, as the wavelength increases to infinity, both the phase and group velocities approach zero, in inverse proportion to the square root of wavelength. The phase velocity and amplitude of this slow wave are in good agreement with those obtained by the numerical studies on the dynamics of fluid-filled cracks by two-dimensional and three-dimensional finite difference methods. In the past the size of a magma body has been estimated from volcanic tremor periods and the acoustic velocity in the fluid. These estimates should be drastically reduced if the slow wave dominates the tremor. For example, the extremely long-period volcanic tremor, with periods up to 7 s, observed at Mount Aso may be generated by a fluid-filled crack of modest size, a magma body 0.5 m thick and 0.5 km long.

Introduction

Volcanic tremor sometimes precedes an eruption, as in the case of El Chichon in 1982 [Havskov et al., 1983] in which tremor occurred just before an eruption and ended with it. In other cases, however, its occurrence is not followed by an eruption. Thus we need to understand its mechanism better in order to use it as a tool to find out about magmatic conditions inside a volcano.

A tremor can last from a few minutes to several days and is characterized by peaked spectra at frequencies ranging from 0.15 to 10 Hz, which may be explained by the resonance set up in magmatic conduits. Temporal changes of tremor period have been observed on various volcanoes, including Kilauea [Shimozuru et al., 1966; Aki and Koyanagi, 1981], Mount Aso [Kubotera, 1974], Sakurajima [Kamo et al., 1977], Mount Etna [Schick et al., 1982], and Mount St. Helens [Fehler, 1983], in support of the idea that the spectral peaks are associated with the source effect rather than the propagation path effect.

Fehler [1983] analyzed data recorded at Mount St. Helens and found that tremor and so called "long-period events" share the same peaked spectra. This led him to suggest that the tremor consisted of a sequence of randomly occurring long-period events. This idea, which was first proposed by Latter [1979] for the tremor at Ruapehu and Ngauruhoe, New Zealand, and has been supported by other workers [Seidl et al., 1981; Fehler and Chouet, 1982; McNutt, 1986], was well demonstrated by Fehler [1983]. Recently, Bame and Fehler [1986] showed that the first events which occur during hydraulic fracturing in virgin rock are long-period events. These observations provide an important link between volcanic tremor and hydraulic fracturing of rock.

Since Sassa [1935] first considered a magma-filled crack for explaining various observations at Mount Aso, numerous models have been developed to interpret volcanic tremor (see Chouet et al. [1987] for the latest review on the subject). In the fluid-driven crack models first studied by Aki et al. [1977], the fluid did not support acoustic waves and simply behaved like a cushion to the vibration of the crack walls. Therefore the observed long duration of the long-period event could not be simulated because of the weak resonance and strong radiation loss. Although several models considering unsteady fluid flow have been proposed [St. Lawrence and Qamar, 1979; Ferrick et al., 1982], the coupling between the fluid and the surrounding elastic solid was not sufficiently analyzed to lead to quantitative results that can be compared with seismic observations. Recently, Chouet [1985, 1986] and Chouet and Julian [1985] have developed models in which the fluid dynamics and seismic radiation are considered to the extent that the acoustic vibration in the fluid and its coupling with the surrounding solid are fully analyzed. In these studies on dynamics of a fluid-filled crack the equations of motion for the fluid are solved simultaneously with those for the elastic solid. They found, among other things, that the resonant period of a fluid-filled crack can be much longer than expected from the acoustic vibration of fluid, because of the existence of very slow waves which Chouet [1986] called "crack waves." The discovery of crack waves may have important implications for the interpretation of volcanic tremor. For example, the puzzle of a tremor with a period as long as 7 s reported by Sassa [1935] at Mount Aso, which required a huge magma reservoir as the resonator may be resolved because the low velocity of crack wave allows a more realistic size of magma body to generate a very long resonance period. Their numerical approach, however, tends to obscure the causal relationship between the observed motion and the model parameters. We decided to start with the simplest case in order to isolate important factors involved in the phenomena and chose the study of normal modes in a fluid layer sandwiched between two elastic half-spaces.

Normal modes in fluid-solid systems have been investigated by many authors. Because of their considerable geophysical interest, two classes of models have been intensively studied: a fluid layer overlying a solid elastic half-space [Stoneley, 1926; Pekeris, 1948; Press and Ewing, 1950; Biot, 1952a; Tolstoy and Clay, 1966], and a fluid-filled borehole [Biot, 1952b; Cheng and Toksoz, 1981; White, 1983].

Normal modes in a fluid layer sandwiched between two homogeneous elastic half-spaces, however, have not attracted much attention except in the work by Paillet and White [1982], who used such a model as a simple approximation to a fluid-filled borehole. In the first part of this paper, following Biot [1952b], who studied seismic waves in the fluid-filled borehole, we derive the equation of dispersion to determine the phase velocities and the eigenfunctions for a given normal mode. We show that both phase and group velocities decrease in inverse proportion to the square root of wavelength and become zero for infinite wavelength. Then using Saito's [1967] method for surface wave excitation, we calculate the amplitude of a mode generated by an explosive source in the fluid layer and compare our results with the numerical results obtained by Chouet's [1986] study of the dynamics of a three-dimensional fluid-filled crack.

The Equation of Motion and Boundary Conditions

Consider a fluid layer of thickness h lying between two elastic half-spaces bounded by the horizontal planes $z = -h/2$ and $z = h/2$, where z is the vertical axis. Our first objective is to determine the dispersion equation for normal modes trapped in the fluid layer. The horizontal and vertical displacement components for the fluid are given in terms of the potential ϕ_f by

$$u_f = \frac{\partial \phi_f}{\partial x}$$
$$w_f = \frac{\partial \phi_f}{\partial z} \tag{1}$$

where ϕ_f satisfies the wave equation

$$\nabla^2 \phi_f = \frac{1}{c^2} \frac{\partial^2 \phi_f}{\partial t^2} \tag{2}$$

t is time, and c is the acoustic wave velocity in the fluid. For waves propagating in the x direction, the solution ϕ_f may be written in the form

Paper number 6B6280.
0148-0227/87/006B-6280$05.00

$$\phi_f = \left(Ae^{i\nu z} + Be^{-i\nu z}\right) e^{i(k_x x - \omega t)} \tag{3a}$$

for $k^2 = (\omega^2/c^2) > k_x^2$ and $\nu^2 = k^2 - k_x^2$, and

$$\phi_f = \left(Ae^{\nu z} + Be^{-\nu z}\right) e^{i(k_x x - \omega t)} \tag{3b}$$

for $k^2 = (\omega^2/c^2) < k_x^2$ and $\nu^2 = k_x^2 - k^2$, and A and B have dimensions of length squared.

The fluid pressure is given by

$$p = -\rho_f \frac{\partial^2 \phi_f}{\partial t^2} \tag{4}$$

ρ_f being the fluid density.

We consider two cases; in one the perturbation of pressure is symmetric, in the other antisymmetric with respect to z. In the following, the superscript S refers to the symmetric mode and corresponds to the upper sign, while the subscript A refers to the antisymmetric mode and corresponds to the lower sign. Putting $\epsilon = \omega/ck_x = v/c$ where v is the horizontal phase velocity of the wave, we have

for $\epsilon > 1$

$$\phi_f \overset{S}{A} = A\left(e^{ik_x\sqrt{\epsilon^2-1}z} \pm e^{-ik_x\sqrt{\epsilon^2-1}z}\right) e^{i(k_x x - \omega t)} \tag{5a}$$

for $\epsilon < 1$

$$\phi_f \overset{S}{A} = A\left(e^{k_x\sqrt{1-\epsilon^2}z} \pm e^{-k_x\sqrt{1-\epsilon^2}z}\right) e^{i(k_x x - \omega t)} \tag{5b}$$

Therefore from equations (1), (4), and (5) the ratio of the pressure to the vertical displacement at $z = \pm h/2$ for symmetric (upper sign) and antisymmetric (lower sign) modes can be written

for $\epsilon > 1$

$$\frac{p}{w_f}\Big]_{z=\pm\frac{h}{2}} \overset{S}{A} = \pm\frac{\rho_f\omega^2 \mathrm{sign}(z)}{k_x\sqrt{\epsilon^2-1}} \begin{pmatrix}\cot\\ \tan\end{pmatrix}\left(\sqrt{\epsilon^2-1}\frac{h}{2}k_x\right)$$

for $\epsilon < 1$

$$\frac{p}{w_f}\Big]_{z=\pm\frac{h}{2}} \overset{S}{A} = \frac{\rho_f\omega^2 \mathrm{sign}(z)}{k_x\sqrt{1-\epsilon^2}} \begin{pmatrix}\coth\\ \tanh\end{pmatrix}\left(\sqrt{1-\epsilon^2}\frac{h}{2}k_x\right)$$

where cot and tan apply to the symmetric and antisymmetric modes respectively.

The horizontal and vertical displacement components in the P-SV problem for an elastic solid are given by

$$\begin{aligned} u &= \frac{\partial\phi}{\partial x} - \frac{\partial\psi}{\partial z} \\ w &= \frac{\partial\phi}{\partial z} + \frac{\partial\psi}{\partial x} \end{aligned} \tag{6}$$

where ϕ and ψ are the potentials of compressional and shear waves which satisfy the wave equations:

$$\begin{aligned} \nabla^2\phi &= \frac{1}{\alpha^2}\frac{\partial^2\phi}{\partial t^2} \\ \nabla^2\psi &= \frac{1}{\beta^2}\frac{\partial^2\psi}{\partial t^2} \end{aligned} \tag{7}$$

with α and β being the velocities of compressional and shear waves in the solid.

These equations have solutions of the form

$$\begin{aligned} \phi &= \phi_o e^{-l_c|z|}\left(e^{ik_x x} + e^{-ik_x x}\right) e^{-i\omega t} \\ \psi &= \psi_o e^{-l_s|z|}\left(e^{ik_x x} - e^{-ik_x x}\right) e^{-i\omega t} \end{aligned} \tag{8}$$

where

$$\begin{aligned} l_c &= \sqrt{k_x^2 - \frac{\omega^2}{\alpha^2}} \\ l_s &= \sqrt{k_x^2 - \frac{\omega^2}{\beta^2}} \end{aligned}$$

The tangential and normal components of traction acting on a plane perpendicular to the z axis are

$$\begin{aligned} \tau_{zx} &= 2\mu\frac{\partial^2\phi}{\partial x\partial z} + \mu\left(\frac{\partial^2\psi}{\partial x^2} - \frac{\partial^2\psi}{\partial z^2}\right) \\ \tau_{zz} &= \lambda\nabla^2\phi + 2\mu\left(\frac{\partial^2\phi}{\partial z^2} - \frac{\partial^2\psi}{\partial x\partial z}\right) \end{aligned} \tag{9}$$

where λ and μ are the Lamé moduli of the solid.

Applying the boundary condition that the shear stress must vanish at the fluid-solid interfaces:

$$\tau_{zx}]_{z=\pm\frac{h}{2}} = 0 \tag{10}$$

we obtain a relation between ϕ_o and ψ_o:

$$\frac{\phi_o}{\psi_o} = \mathrm{sign}(z)\frac{i(2-\epsilon_s^2)}{2\sqrt{1-\epsilon_c^2}} e^{\frac{h}{2}(l_c - l_s)} \tag{11}$$

with $\epsilon_s = v/\beta$ and $\epsilon_c = v/\alpha$. Using the above relations, the ratio of the stress component τ_{zz} to the vertical displacement w at $z = \pm h/2$ can be written as

$$\frac{\tau_{zz}}{w}\Big]_{z=\pm\frac{h}{2}} = \mathrm{sign}(z)\rho_s\frac{\beta^2 k_x}{\epsilon_s^2}\left(\frac{(2-\epsilon_s^2)^2}{\sqrt{1-\epsilon_c^2}} - 4\sqrt{1-\epsilon_s^2}\right) \tag{12}$$

where ρ_s is the density of the solid.

The Equation of Dispersion

The vertical component of the traction and the displacement must be continuous at the fluid-solid interfaces. Following Biot [1952b] we define a mechanical impedance as the ratio of stress to displacement and match the impedances at the fluid-solid interfaces $z = \pm h/2$:

$$\frac{p}{w_f} = \frac{-\tau_{zz}}{w} \tag{13}$$

From this, four dispersion equations for waves with horizontal phase velocity $v = \omega/k_x$ are obtained. For $\epsilon > 1$,

$$\begin{pmatrix}\cot\\ \tan\end{pmatrix}\left[\sqrt{\epsilon^2-1}\left(\frac{hk_x}{2}\right)\right] \overset{S}{A} = \pm\frac{\rho_s}{\rho_f}\frac{\sqrt{\epsilon^2-1}}{\epsilon_s^4}\left(\frac{(2-\epsilon_s^2)^2}{\sqrt{1-\epsilon_c^2}} - 4\sqrt{1-\epsilon_s^2}\right) \tag{14a}$$

and for $\epsilon < 1$

$$\begin{pmatrix}\coth\\ \tanh\end{pmatrix}\left[\sqrt{1-\epsilon^2}\left(\frac{hk_x}{2}\right)\right] \overset{S}{A} = -\frac{\rho_s}{\rho_f}\frac{\sqrt{1-\epsilon^2}}{\epsilon_s^4}\left(\frac{(2-\epsilon_s^2)^2}{\sqrt{1-\epsilon_c^2}} - 4\sqrt{1-\epsilon_s^2}\right) \tag{14b}$$

For given values of the three ratios ρ_s/ρ_f, ϵ_s, and Poisson ratio σ, which is related to the velocities α and β by the equation

$$\frac{\epsilon_c^2}{\epsilon_s^2} = \frac{2(1-\sigma)}{1-2\sigma} \tag{15}$$

the phase velocity can be determined as a function of wavelength. This can be simply done using a bisection method. The solution of the above equations when $\rho_s/\rho_f = 2.5$, $\beta/c = 1.5$, and $\sigma = 0.25$ is given in Figure 1.

The antisymmetric group (for which the plane $z = 0$ is a constant-pressure surface) contains all the modes which can be observed in a fluid layer overlying a solid half-space such as the ocean and has been investigated by numerous authors, for example, Biot [1952a] and Tolstoy [1954]. It does not need further discussion here.

The Existence of Very Slow Waves

In the symmetric group, the most important feature is the fundamental mode, which exists for all wavelengths. The phase velocity of this mode is lower than the acoustic velocity of the fluid for

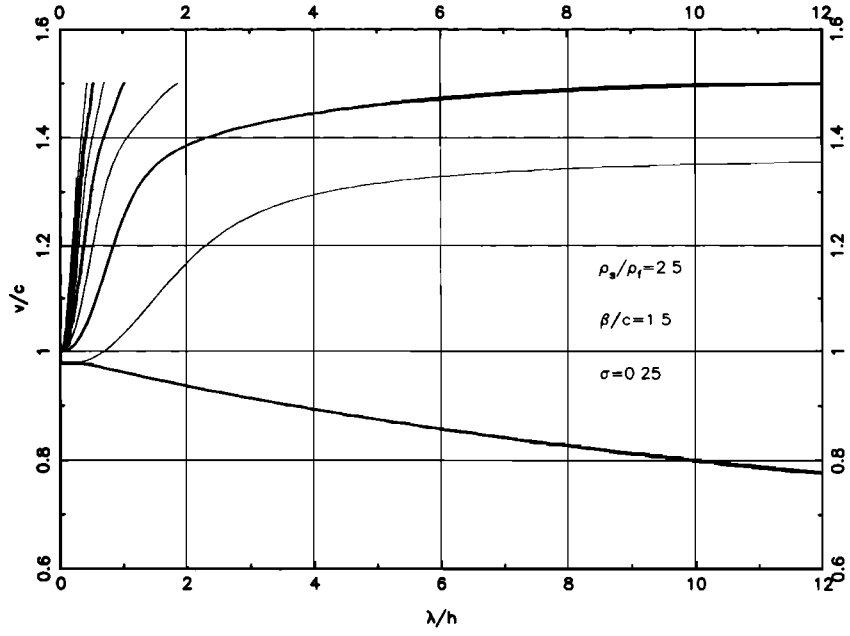

Fig. 1. Phase velocity divided by acoustic velocity plotted as a function of the wavelength divided by the layer thickness. Branches of the symmetric group are represented by bold lines and those of the antisymmetric group by thin lines

all wavelengths and decreases as the wavelength increases. At high frequencies this slow wave becomes the Stoneley wave propagating along the fluid-solid interface. For this reason, it is comparable to the tube wave studied by Biot [1952b], but as the wavelength tends to infinity, the velocity approaches zero according tc

$$\lim_{\lambda\to\infty}\left(\frac{v}{c}\right)^2 = 2\left(\frac{\beta^2}{c^2}\right)\left(1-\frac{\beta^2}{\alpha^2}\right) \cdot\left[\frac{\lambda}{\pi h}\frac{\rho_f}{\rho_s} - \left(\frac{\beta^2}{\alpha^2}\left(2-\frac{\beta^2}{\alpha^2}\right) + 2\frac{\beta^2}{c^2}\left(\frac{\beta^2}{\alpha^2}-1\right) - \frac{1}{2}\right)\right]^{-1} \quad (16)$$

varying inversely with the square root of the wavelength (Figure 2) unlike the tube wave, for which the velocity approaches a finite value.

One consequence of this slow-velocity branch is that resonance at a long period may be possible for a small fluid-filled crack. For example, for a fluid-filled crack of length 1 *km* and thickness 0.5 *m*, with the parameters $\rho_s/\rho_f = 2.5$, $\beta/c = 1.5$, $\sigma = 0.25$, and $c = 2$ km/s, the half wavelength equal to the crack length will correspond to a period of 10 *s*, which is 10 times the period of resonance of acoustic waves in the fluid. Sassa [1935] made some broadband measurements on Mount Aso using long-period seismographs (Galitzin type, $T_0 = 8$ s) within 1 km from the crater. He recorded tremor associated with the magmatic activity, which he called "tremor of the second kind," and which has a period ranging between 3.5 and 7 s. Kubotera [1974] interpreted this tremor as due to the vibrations of a spherical magma chamber. He found, assuming the acoustic velocity is 2 km/s, that the chamber diameter must range between 4 and 8 km to explain the observed period. Using another model, the fluid-driven crack model of Chouet [1981], one concludes that the total crack length should be at least of the order of 4 km. Since the previous estimations were based on the acoustic velocity in the

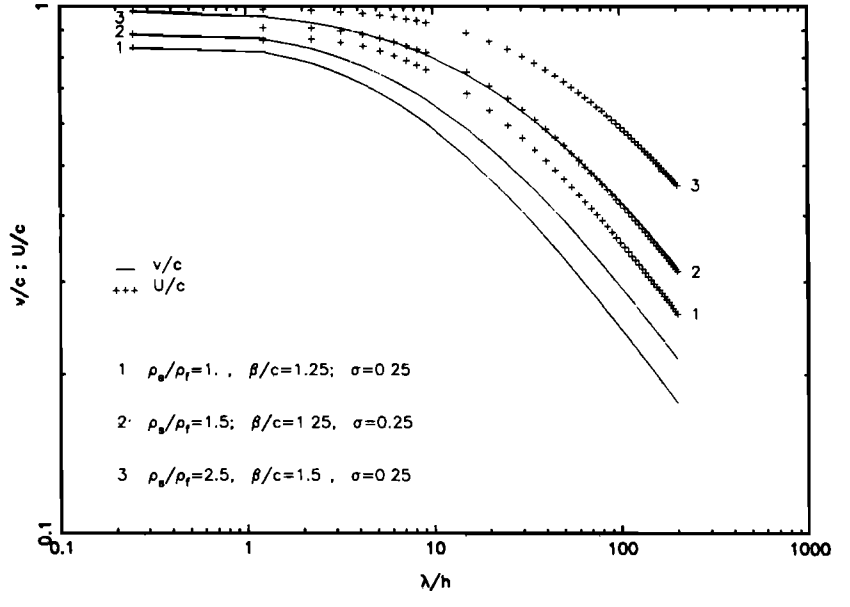

Fig. 2. Phase and group velocity, v and U, of the fundamental symmetric mode as a function of wavelength for three different sets of medium characteristics.

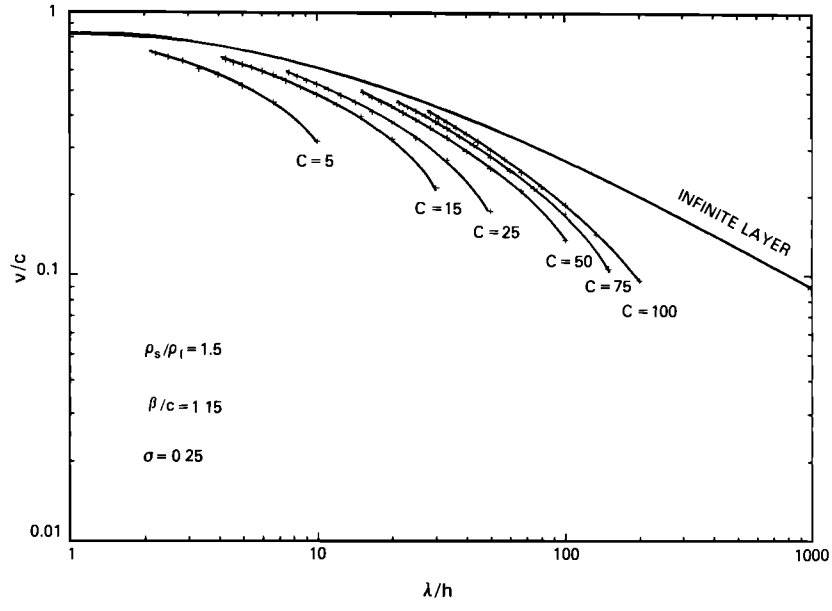

Fig. 3. Comparison of the phase velocity of the fundamental symmetric mode with that inferred from the numerical results on apparent period and wavelength, obtained by Chouet [1986] for a crack of finite length and for different values of the stiffness factor C which is attached to each curve.

magma, the slow wave will allow a drastic reduction in the estimate of magma body size. The long period of volcanic tremor up to 7 s observed at Mount Aso may be explained by a modest-sized magma body 0.5 km long and 0.5 m thick.

The existence of this slow wave has been demonstrated in Chouet's [1986] studies on the dynamics of a fluid-filled crack excited by the rupture of a barrier, using a three-dimensional finite difference method. He observes slow waves that he calls "crack waves" and plots in his Figure 17, the dispersion curves v/c, for different values of the stiffness factor C, against the dimensionless wavelength λ/L, L being the length of the crack. The stiffness factor, introduced by Aki et al. [1977], is an important parameter controlling the dynamics of fluid-filled cracks and is defined as

$$C = \frac{bL}{\mu h}$$

where b is the bulk modulus of the fluid, μ is the rigidity of the solid, L is the length of the crack, and h is the crack thickness. For the case $\rho_s/\rho_f = 1.5$, $\beta/v = 1.15$, $\sigma = 0.25$, Figure 3 compares the phase velocity of the fundamental symmetric mode with that estimated from Chouet's numerical results on apparent period and wavelength. The result obtained for a crack of infinite length appears to lie at a natural extrapolation of increasing crack stiffness factor which is proportional to crack length. It is interesting to note that for each run of the finite difference calculation, v/c is the lowest for the longest wavelength ($\lambda = L$) and is roughly one half of the asymptotic value for short wavelengths. Thus the ratio v/c to be used for calculation of resonance ($\lambda = L$) should be about one half of the value given by the analytic curve which appears to be asymptotic to the numerical results at short wavelengths.

The Motion-Stress Vector

To get more insight into the motion set up by this slow wave, we compute its eigenfunctions. Since the slow wave (fundamental mode) has a particle motion similar to that of Rayleigh waves, using the notation of Aki and Richards [1980], the displacement and stress components can be written

$$\begin{aligned} u &= y_1(k_x, z, \omega)\exp(i(k_x x - \omega t)) \\ w &= iy_2(k_x, z, \omega)\exp(i(k_x x - \omega t)) \\ \tau_{xz} &= y_3(k_x, z, \omega)\exp(i(k_x x - \omega t)) \\ \tau_{zz} &= iy_4(k_x, z, \omega)\exp(i(k_x x - \omega t)) \end{aligned} \tag{17}$$

where (y_1, y_2, y_3, y_4) is called the motion-stress vector. Taking into account the continuity of y_2 at the fluid-solid interface one may express the four components of this motion-stress vector as a function of only one undetermined constant. The group velocity may then be written in the form [Aki and Richards, 1980, p. 291]

$$U = \frac{I_2 + I_3/2k_x}{vI_1} \tag{18}$$

where the energy integrals are

$$\begin{aligned} I_1 &= \frac{1}{2}\int_{-\infty}^{+\infty} \rho\,(y_1^2 + y_2^2)\,dz \\ I_2 &= \frac{1}{2}\int_{-\infty}^{+\infty} \left[(\lambda + 2\mu)\,y_1^2 + \mu y_2^2\right] dz \\ I_3 &= \int_{-\infty}^{+\infty} \left(\lambda y_1 \frac{dy_2}{dz} - \mu y_2 \frac{dy_1}{dz}\right) dz \end{aligned} \tag{19}$$

and can be evaluated analytically to obtain the group velocity as a function of the wavelength. Since the slope of the velocity curve as a function of the wavelength is negative, the group velocity is always greater than the phase velocity. At large wavelengths, where the phase velocity is proportional to the inverse of the square root of the wavelength, the group velocity equals three halves of the phase velocity and thus tends also to zero when the wavelength goes to infinity.

Figure 4 shows the four components of the motion-stress vector for the fundamental symmetric (Figure 4a) and antisymmetric modes (Figure 4b) for the values λ/h ranging from 0 025 to 11 025, $\rho_s/\rho_f = 2.5$, $\beta/c = 1.5$, and $\sigma = 0.25$. In these figures the liquid layer lies between $z/h = -0.5$ and 0.5. The amplitudes of the displacement functions y_1 and y_2 are normalized to a unit value of y_2 at the fluid-solid interface. Those of the traction functions, y_3 and y_4, are normalized to a unit vertical traction at the same interface. In Figure 4b, when the phase velocity reaches the acoustic velocity, there is a phase change that inverts the sign of the eigenfunctions.

In Figure 4a the fundamental symmetric mode shows a very large horizontal displacement y_1 inside the fluid layer. Furthermore, this motion increases with the wavelength, and for large wavelengths the whole section of the fluid layer is displaced as a whole.

Excitation of the Slow Wave by an Explosive Source in the Fluid Layer

So far we have been concerned only with the free waves propagating along the interface. To calculate absolute amplitudes, we

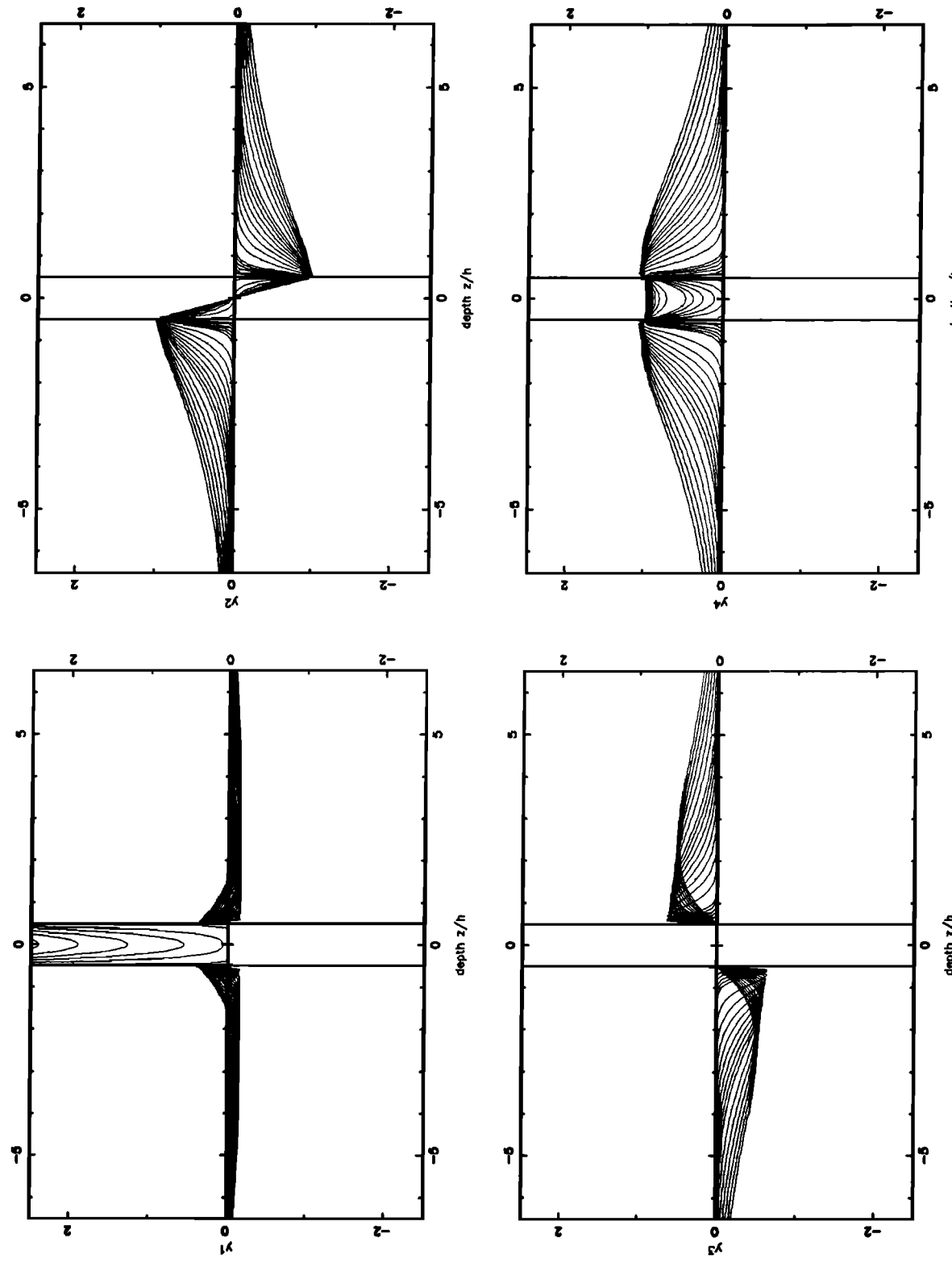

Fig. 4a. For the symmetric fundamental mode, distribution of displacement y_1 parallel to the fluid-solid interface, displacement y_2 perpendicular to it, shear stress y_3 acting on a plane parallel to the interface, and normal stress y_4 acting on it. The different curves correspond to different wavelengths ranging from 0.025h to 11.025h. The medium parameters are the same as in Figure 1.

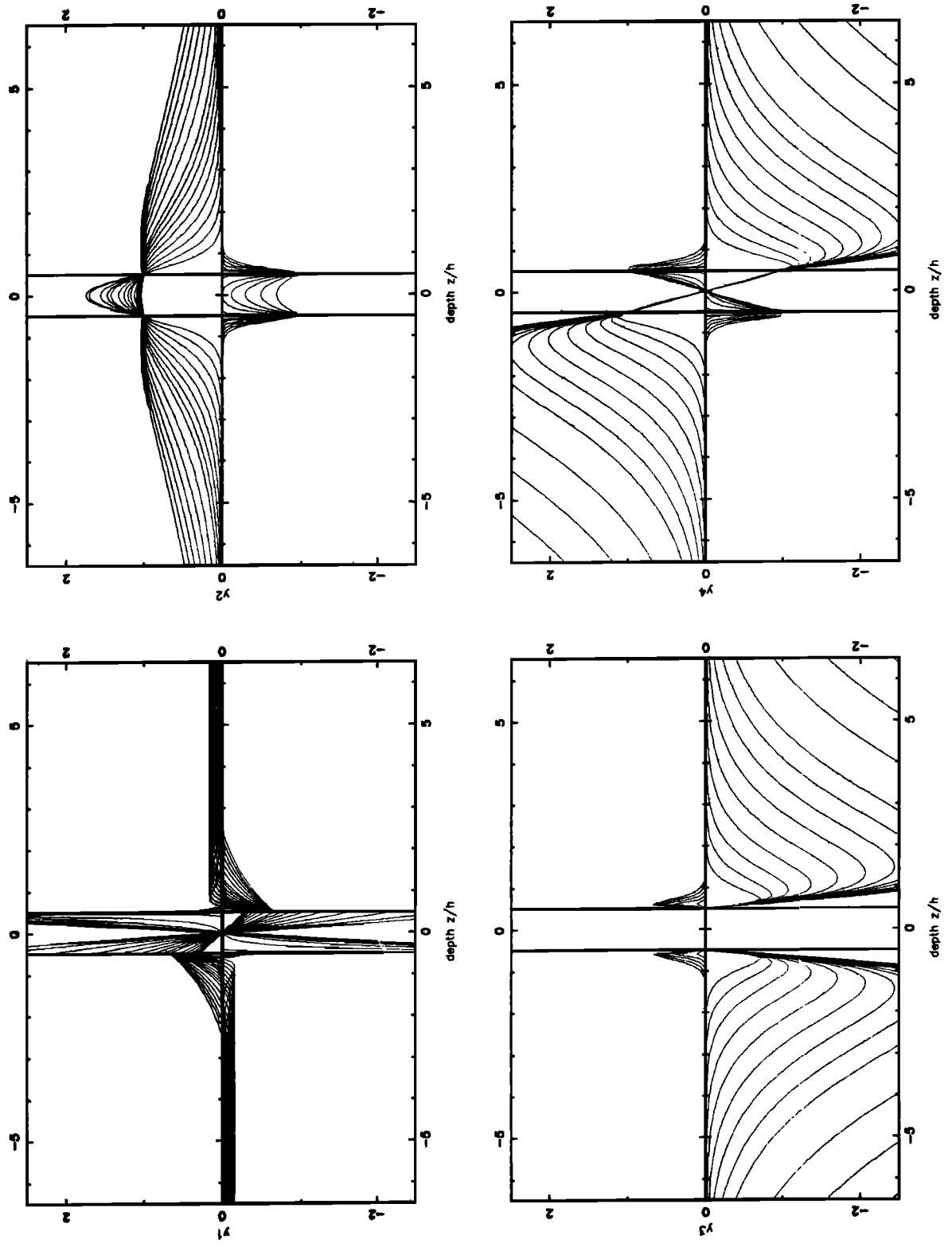

Fig. 4b. Same as Figure 4a for the fundamental mode of the antisymmetric group.

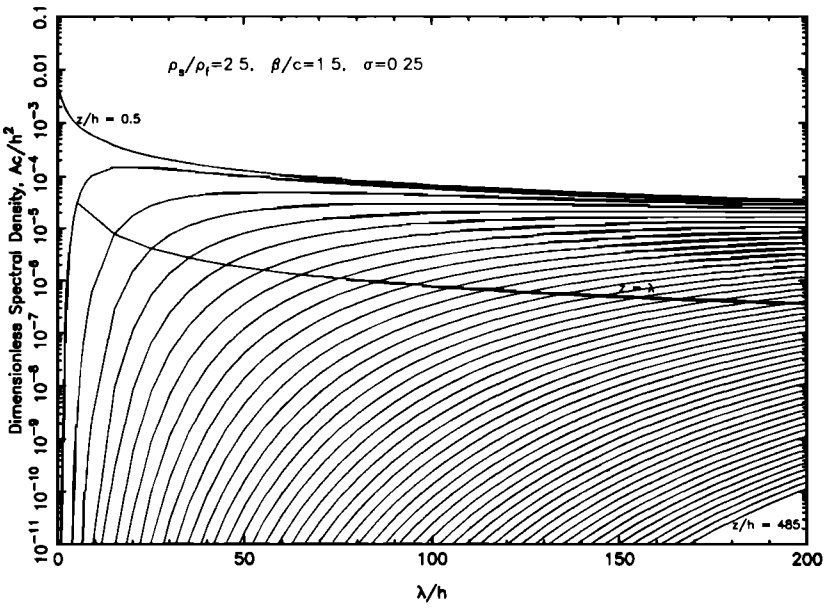

Fig. 5. Dimensionless amplitude spectral density of the vertical displacement as a function of the dimensionless wavelength λ/h, at a horizontal distance $r = 1000$h. The upper line corresponds to $z = h/2$ (the fluid-solid interface). The other curves correspond to depths varying from 5h to 485h, at intervals of 10h. The source considered is an explosion located in the middle of the fluid layer at ($r = 0., z = 0.$). Also drawn in this figure is the curve of the spectral amplitude at $z = \lambda$.

consider an explosive point source located at $x = y = z = 0$, in the middle of the fluid layer. The moment tensor is then reduced to the three equal diagonal elements, $M_{xx} = M_{yy} = M_{zz} = M_o(t)$.

According to Aki and Richards [1980, p. 317], if we assume a step function for $M_o(t)$, using cylindrical coordinates (r, z, ϕ), the Fourier transform of the vertical displacement due to the fundamental symmetric mode is given by the expression

$$w(r,z,\omega) = M_o \frac{y_2(z)}{8vUI_1}\left(\frac{2}{\pi k_x r}\right)^{\frac{1}{2}}\left(\frac{-1}{i\omega}\right) \cdot \exp\left[i\left(k_x r + \frac{\pi}{4}\right)\right]\left[k_x y_1(0) + \frac{dy_2}{dz}|_0\right] \quad (20)$$

In order to facilitate the presentation of our result in a diagram, we use the non-dimensional variables defined by

$$z = z^* h \qquad \omega = \frac{\omega^* c}{h} \qquad v = v^* c$$
$$\rho = \rho^* \rho_f \qquad M_o = M_o^* \rho_f h^3 c^2 \quad (21)$$

and the dimensionless amplitude spectral density is obtained as

$$A = A^* \frac{h^2}{c} \quad (22)$$

Figure 5 shows the dimensionless amplitude spectral density of

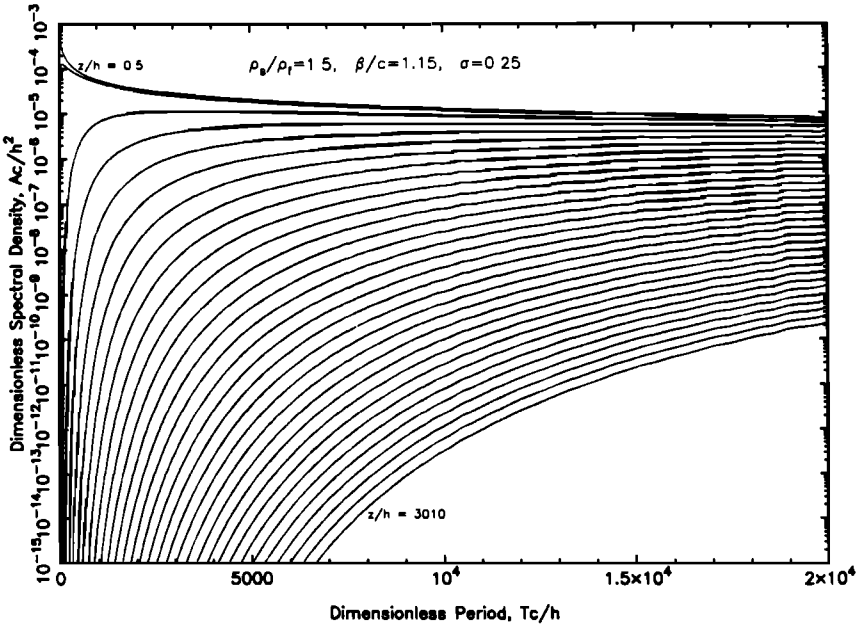

Fig. 6. Dimensionless amplitude spectral density of the vertical displacement as a function of the dimensionless period at distance $r = 1000$h. The upper line corresponds to $z = h/2$. The other curves correspond to depths varying from 10h to 3010h, at intervals of 100h. The source considered is the same as in Figure 5.

the vertical displacement, for $M_o^* = 1$, as a function of the dimensionless wavelength with the same set of ratios as in Figure 4, at the horizontal distance $r = 1000$ h and for depths z between $h/2$ (the fluid-solid interface) and 485 h. Also drawn in this figure is the curve of the spectral amplitude at $z = \lambda$. The amplitude decreases by about a factor of 100 from the edge of the crack to a vertical distance equal to the wavelength. Thus our trapped mode is difficult to observe at a vertical distance greater than a wavelength. If the crack is finite, however, the strong horizontal motion propagating in the fluid layer may provide an important source of radiation which can be observed at large distances. In order to compare the amplitude of the displacement at the fluid-solid interface with those obtained by Chouet [1986] for the crack wave, we have plotted (Figure 6) the amplitude spectral density as a function of the dimensionless period,

$$T = T^* \frac{h}{c} \tag{23}$$

for the case $\rho_s/\rho_f = 1.5$, $\beta/c = 1.155$, and $\sigma = 0\ 25$, which is identical to the medium he considered. For a stiffness factor $C = 100$, if we assume the crack length $L = 100$ m and $b/\mu = 0.5$, then the crack he considered has a barrier area $S = 12.5$ m^2. Taking an applied excess pressure $P = 100$ bars and an acoustic velocity of 2 km/s, from Figures 15 and 16 of Chouet [1986] we can evaluate the amplitude spectral density of normal displacement at the crack surface, due to the crack wave. The estimated amplitude spectral density is of the order of $W = 9 \times 10^{-5}$ cm s at a period $T = 0.52$ s. Considering an equivalent diagonal element of moment $M_o = PSh$ [Aki and Richards, 1980, p. 60] and the same period, after correction of the geometrical spreading, we find that the amplitude spectral density equals 1×10^{-5} cm s. We consider this agreement to be satisfactory in view of the extremely simple and rapid calculation involved in (20) as compared with Chouet's finite difference calculation.

Summary

We found that a very slow wave, trapped in a fluid layer sandwiched between two elastic half-spaces, exhibits extraordinary behavior; both phase and group velocities tend to zero as the wavelength goes to infinity. This result agrees with Chouet's [1986] result on the phase velocity of the so-called crack wave obtained by a three-dimensional finite difference calculation on the dynamics of a fluid-filled finite crack. Although this slow wave is difficult to observe at distances greater than a wavelength from the fluid layer for the case of the infinite layer, reflection at the crack tip should provide an important source of radiation in the case of a finite crack. Our estimation of the amplitude of the normal displacement at the fluid-solid interface is also in good agreement with Chouet's [1986] results. This wave may play an important role in the long-period events observed in volcanoes and geothermal areas and may explain their signal duration and low frequencies. Also the estimated dimensions of the source of long-period events can be drastically reduced from the case in which the resonance period was attributed to acoustic waves in the fluid. For example, the long-period tremor observed by Sassa [1935] at Mount Aso in 1933, with periods ranging from 3.5 to 7 s, may be explained by a modest-sized magma body, 0.5 m thick and 0.5 km long. The existence of this wave may also suggest that we are not recording and analyzing the tremor in the optimal range of frequencies. If we instrument volcanoes with seismographs more sensitive to long-period motion, we may observe slow waves more effectively and be able to use them to find the geometrical and mechanical properties of magma bodies. For this purpose, we need to study further the effects of material properties, such as viscosity, on the characteristics of tremors.

Acknowledgments. We would like to thank Bernard Chouet for providing us his results in advance and for helpful discussions. We also gratefully appreciate the careful reviews by Mike Fehler and Bruce Julian. This work was supported by the Department of Energy under contract DE FG03 85ER 13336.

References

Aki, K., and R. Koyanagi, Deep volcanic tremor and magma ascent mechanism under Kilauea, Hawaii, J. Geophys. Res., 86, 7095–7109, 1981.

Aki, K., and P. G. Richards, Quantitative Seismology: Theory and Methods, W. H. Freeman, San Francisco, 1980.

Aki, K., M. Fehler, and S Das, Source mechanism of volcanic tremor: Fluid-driven crack models and their application to the 1963 Kilauea eruption, J. Volcanol. Geotherm. Res., 2, 259–287, 1977.

Bame, D. A., and M. C. Fehler, Observations of long-period earthquakes accompanying hydraulic fracturing, Geophys. Res. Lett., 13, 144–152, 1986.

Biot, M. A., The interaction of Rayleigh and Stoneley waves in the ocean bottom, Bull. Seismol. Soc. Am., 42, 82–92, 1952a.

Biot, M. A., Propagation of elastic waves in a cylindrical bore containing a fluid, J. Appl. Phys., 23, 997–1005, 1952b.

Cheng, H. C., and M. N. Toksoz, Elastic wave propagation in a fluid-filled bore-hole and synthetic acoustic logs, Geophysics, 46, 1042–1053, 1981.

Chouet, B., Ground motion in the near field of a fluid-driven crack and its interpretation in the study of shallow volcanic tremor, J. Geophys. Res., 86, 5985–6016, 1981.

Chouet, B., Excitation of a buried magmatic pipe: A seismic source model for volcanic tremor, J. Geophys. Res., 90, 1881–1893, 1985.

Chouet, B., Dynamics of a fluid driven crack in three dimensions by the finite difference method, J. Geophys. Res., 91, 13,967–13,992, 1986.

Chouet, B., and B. R. Julian, Dynamics of an expanding fluid-filled crack, J. Geophys. Res., 90, 11,184–11,198, 1985.

Chouet, B., R. Koyanagi, and K. Aki, The origin of volcanic tremors in Hawaii, II, Theory and discussion, U.S. Geol. Surv. Prof. Pap., 1350, 1987.

Fehler, M. C., Observation of volcanic tremor at Mount St. Helens volcano, J. Geophys. Res., 88, 3476–3484, 1983.

Fehler, M., and B. Chouet, Operation of a digital seismic network on Mount St. Helens volcano and observations of long-period seismic events that originate under the volcano, Geophys. Res. Lett., 9, 1017–1020, 1982.

Ferrick, M. G., A. Qamar, and W. F. St. Lawrence, Source mechanism of volcanic tremor, J. Geophys. Res., 87, 8675–8683, 1982.

Havskov, J., S. De la Cruz-Reyna, S. K. Singh, F. Medina, and C. Gutierrez, Seismic activity related to the March–April, 1982 eruptions of El Chichon volcano, Chiapas, Mexico, Geophys. Res. Lett., 10, 293–296, 1983.

Kamo, K., T. Furuzawa, and J. Akamatsu, Some natures of volcanic micro-tremors at the Sakurajima volcano, Bull. Volcanol. Soc. Jpn., 22, 41–58, 1977.

Kubotera, A., Volcanic tremors at Aso volcano, in Physical Volcanology, edited by L. Civetta, P. Gasparini, G. Luongo, and A. Rapolla, pp. 29–47, Elsevier, Amsterdam, 1974.

Latter, J. H., Volcanological observations at Tongariro National Park, 2, Types and classification of volcanic earthquakes, 1976–1978, Rep. 150, 60 pp., N. Z. Dep. of Sci. and Ind. Res. Geophys. Div., Wellington, New Zealand, 1979.

McNutt, S. R., Observations and analysis of B-type earthquakes, explosions, and volcanic tremor at Pavlov volcano, Alaska, Bull. Seismol. Soc. Am., 76, 153–175, 1986.

Paillet, F. L., and J. E. White, Acoustic modes of propagation in the borehole and their relationship to rock properties, Geophysics, 47, 1215–1228, 1982.

Pekeris, C. L., Theory of propagation of explosive sound in shallow water, Mem. Geol. Soc Am., 27, 1948.

Press, F., and M. Ewing, Propagation of explosive sound in a liquid layer overlying a semi-infinite elastic solid, Geophysics, 15, 426–467, 1950.

Saito, M., Excitation of free oscillations and surface waves by a point source in a vertically heterogeneous earth, J. Geophys. Res., 72, 3689–3699, 1967.

Sassa, K., Volcanic micro-tremors and eruption-earthquakes, Mem. Coll. Sci. Univ. Kyoto, Ser. A, 18, 255–293, 1935.

Schick, R., G. Lombardo, and G. Patane, Volcanic tremors and shocks associated with the eruptions at Etna (Sicily), September 1980, J. Volcanol. Geotherm. Res., 14, 261–279, 1982.

Seidl, D., R. Schick, and M. Riuscetti, Volcanic tremor at Etna: A model for hydraulic origin, Bull. Volcanol., 44, 3–56, 1981.

Shimozuru, D., K. Kamo, and W. Kinoshita, Volcanic tremor of Kilauea volcano, Hawaii, during July–December, 1963, Bull. Earthquake Res. Inst. Univ. Tokyo, 44, 1093–1133, 1966.

St. Lawrence, W., and A. Qamar, Hydraulic transients: A seismic source in volcanoes and glaciers, Science, 203, 654–656, 1979.

Stoneley, R., The effect of the ocean on Rayleigh waves, Month. Not. Roy. Astron. Soc. Geophys. Suppl., 1, 349–356, 1926.
Tolstoy, I., Dispersive properties of a fluid layer overlying a semi-infinite elastic solid, Bull. Seismol. Soc. Am., 44, 493–512, 1954.
Tolstoy, I., and C. S. Clay, Ocean Acoustics: Theory and Experiment in Underwater Sound, McGraw-Hill, New York, 1966.
White, J. E., Underground Sound, Elsevier, New York, 1983.

K. Aki and V. Ferrazzini, Department of Geological Sciences, University of Southern California, University Park, Los Angeles, CA 90089.

(Received September 8, 1986;
revised January 20, 1987;
accepted February 9, 1987.)